Nonlinearity **11** (1998) 1015–1035. Printed in the UK PII: S0951-7715(98)90404-2

Harmonic inversion as a general method for periodic orbit quantization

Jörg Main†, Vladimir A Mandelshtam‡, Günter Wunner§ and Howard S Taylor‖

† Theoretische Physik I, Ruhr-Universität Bochum, D-44780 Bochum, Germany
‡ University California Irvine, Department of Chemistry, Los Angeles, CA 92612, USA
§ Institut für Theoretische Physik und Synergetik, Universität Stuttgart, D-70550 Stuttgart, Germany
‖ University of Southern California, Department of Chemistry, Los Angeles, CA 90089, USA

Received 23 December 1997
Recommended by J P Keating

Abstract. In semiclassical theories for chaotic systems, such as Gutzwiller's periodic orbit theory, the energy eigenvalues and resonances are obtained as poles of a non-convergent series $g(w) = \sum_n A_n \exp(\mathrm{i}s_n w)$. We present a general method for the analytic continuation of such a non-convergent series by harmonic inversion of the 'time' signal, which is the Fourier transform of $g(w)$. We demonstrate the general applicability and accuracy of the method on two different systems with completely different properties: the Riemann zeta function and the three-disk scattering system. The Riemann zeta function serves as a mathematical model for a bound system. We demonstrate that the method of harmonic inversion by filter-diagonalization yields several thousand zeros of the zeta function to about 12 digit precision as eigenvalues of small matrices. However, the method is not restricted to bound and ergodic systems, and does not require the knowledge of the mean staircase function, i.e. the Weyl term in dynamical systems, which is a prerequisite in many semiclassical quantization conditions. It can therefore be applied to open systems as well. We demonstrate this on the three-disk scattering system, as a physical example. The general applicability of the method is emphasized by the fact that one does not have to resort to a symbolic dynamics, which is, in turn, the basic requirement for the application of cycle expansion techniques.

PACS numbers: 0365S, 0545, 0230P

1. Introduction

Since the development of *periodic orbit theory* by Gutzwiller [1, 2] it has become a fundamental question as to how individual semiclassical eigenenergies and resonances can be obtained from periodic orbit quantization for classically chaotic systems. A major problem is the exponential proliferation of the number of periodic orbits with increasing period, resulting in a divergence of Gutzwiller's trace formula at real energies and below the real axis, where the poles of the Green's function are located. The periodic orbit sum is a Dirichlet series

$$g(w) = \sum_n A_n \mathrm{e}^{\mathrm{i}s_n w}, \tag{1}$$

where the parameters A_n and s_n are the amplitudes and periods (actions) of the periodic orbit contributions. In most applications equation (1) is absolutely convergent only in the region

$\mathrm{Im}\, w > c > 0$ where c is the entropy barrier of the system, while the poles of $g(w)$, i.e. the bound states and resonances, are located on and below the real axis, $\mathrm{Im}\, w \leqslant 0$. Thus, to extract individual eigenstates, the semiclassical trace formula (1) has to be analytically continued to the region of the quantum poles.

Up to now no general procedure has been known for the analytic continuation of a non-convergent Dirichlet series of the type of equation (1). All existing techniques are restricted to special situations. For bound and ergodic systems the semiclassical eigenenergies can be extracted with the help of a functional equation and the mean staircase function (Weyl term), resulting in a Riemann–Siegel-type formula [3–6]. Alternative semiclassical quantization conditions based on a semiclassical representation of the spectral staircase [7, 8] and derived from a quantum version of a classical Poincaré map [9] are also restricted to bound and ergodic systems.

For systems with a symbolic dynamics the periodic orbit sum (1) can be reformulated as an infinite Euler product, which can be expanded in terms of the cycle length of the symbolic code. If the contributions of longer orbits are shadowed by the contributions of short orbits the cycle expansion technique can remarkably improve the convergence properties of the series and allows us to extract the bound states and resonances of bound and open systems, respectively [10–13]. A combination of the cycle expansion technique with a functional equation for bound systems has been studied by Tanner *et al* [14]. However, the existence of a simple symbolic code is restricted to very few systems, and cycle expansion techniques cannot be applied, e.g. to the general class of systems with mixed regular–chaotic classical dynamics.

In this paper we present a general technique for the analytic continuation and the extraction of poles of a non-convergent series of the type of equation (1). The method is based on *harmonic inversion* by filter-diagonalization. The advantage of this method is that it does not depend on special properties of the system such as ergodicity or the existence of a symbolic dynamics for periodic orbits. It does not even require the knowledge of the mean staircase function, i.e. the Weyl term in dynamical systems. The only assumption we have to make is that the analytic continuation of the Dirichlet series $g(w)$ (equation (1)) is a linear combination of poles $(w - w_k)^{-1}$, which is exactly the functional form of, e.g. a quantum-mechanical response function with real and complex parameters w_k representing the bound states and resonances of the system, respectively. To demonstrate the general applicability and accuracy of our method we will apply it to two systems with completely different properties, first the zeros of the Riemann zeta function [15, 16], as a mathematical model for a bound system, and then the three-disk scattering system as a physical example.

As pointed out by Berry [3] the density of zeros of Riemann's zeta function can be written, in formal analogy with Gutzwiller's semiclassical trace formula, as a non-convergent series, where the 'periodic orbits' are the prime numbers. A special property of this system is the existence of a functional equation which allows the calculation of Riemann zeros via the Riemann–Siegel formula [15–17]. An analogous functional equation for quantum systems with an underlying chaotic (ergodic) classical dynamics has served as the basis for the development of a semiclassical quantization rule for bound ergodic systems [3–6]. The Riemann zeta function has also served as a mathematical model to study the statistical properties of level distributions [17–19]. We will demonstrate that harmonic inversion can reveal the Riemann zeros with extremely high accuracy and with just prime numbers as input data. The most important advantage of our method is, however, its wide applicability, i.e. it can be generalized in a straightforward way to non-ergodic bound or open systems.

Our second example, the three-disk scattering problem, is an open and non-ergodic system. Its classical dynamics is purely hyperbolic, and the periodic orbits can be classified

by a complete binary symbolic code. This system has served as a model for the development of cycle expansion techniques [10, 12, 13]. When applying the harmonic inversion technique to the three-disk scattering system we will highlight the general applicability of our method by not having to make use of its symbolic dynamics in any way.

It is evident that methods invoking special properties of a given system may be more efficient regarding, e.g. the number of periodic orbits required for the calculation of a certain number of poles of the response function $g(w)$ in that particular case. It is not our purpose to compete with the efficiency of such methods. Rather, the advantage of the harmonic inversion technique lies in its wide applicability, which also allows the investigation of systems not possessing special properties. This is demonstrated in this paper by solving two completely different problems, namely the zeros of the Riemann zeta function and the three-disk scattering system, with one and the same method.

This paper is organized as follows. In section 2 we explain the general idea of the method by way of example of the Riemann zeros. This is followed by the derivation of the harmonic inversion method in section 3 and the presentation of numerical results for the Riemann zeros in section 4. The method is extended to the general case of periodic orbit quantization in section 5, and its usefulness and wide applicability is demonstrated for the three-disk scattering system, as a physical example, in section 6.

2. The Riemann zeta function

Our aim is to introduce our method for periodic orbit quantization by harmonic inversion using, as an example, the well-defined problem of calculating zeros of the Riemann zeta function. There are essentially two advantages of studying the zeta function instead of a 'real' physical bound system. First, the Riemann analogue of Gutzwiller's trace formula is exact, as is the case for systems with constant negative curvature [2, 8], whereas the semiclassical trace formula for systems with plane geometry is correct only to first order in $\overline{h}$. This allows a direct check on the precision of the method. Second, no extensive periodic orbit search is necessary for the calculation of Riemann zeros, as the only input data are just prime numbers. It is not our intention to introduce another method for computing Riemann zeros, which, as an objective in its own right, can be accomplished more efficiently by specific procedures. Rather, in our context the Riemann zeta function serves primarily as a mathematical model to illustrate the power of our technique when applied to bound systems.

2.1. General remarks

Before discussing the harmonic inversion method we start by recapitulating a few brief remarks on Riemann's zeta function necessary for our purposes. The hypothesis of Riemann is that all the non-trivial zeros of the analytic continuation of the function

$$\zeta(z) = \sum_{n=1}^{\infty} n^{-z} = \prod_{p} (1 - p^{-z})^{-1}, \qquad (\mathrm{Re}\, z > 1,\ p : \text{primes}) \tag{2}$$

have real part $\frac{1}{2}$, so that the values $w = w_k$, defined by

$$\zeta(\tfrac{1}{2} - \mathrm{i}w_k) = 0, \tag{3}$$

are all real or purely imaginary [15, 16]. The Riemann staircase function for the zeros along the line $z = \frac{1}{2} - \mathrm{i}w$, defined as

$$N(w) = \sum_{k=1}^{\infty} \Theta(w - w_k), \tag{4}$$

i.e. the number $N(w)$ of zeros with $w_k < w$, can be split [3, 15, 16] into a smooth part,

$$\overline{N}(w) = \frac{1}{\pi}\arg\Gamma\left(\frac{1}{4}+\frac{1}{2}\mathrm{i}w\right) - \frac{w}{2\pi}\ln\pi + 1$$
$$= \frac{w}{2\pi}\left(\ln\left\{\frac{w}{2\pi}\right\} - 1\right) + \frac{7}{8} + \frac{1}{48\pi w} - \frac{7}{5760\pi w^3} + \mathcal{O}(w^{-5}), \tag{5}$$

and a fluctuating part,

$$N_{\mathrm{osc}}(w) = -\frac{1}{\pi}\lim_{\eta\to 0}\mathrm{Im}\ln\zeta\left(\frac{1}{2} - \mathrm{i}(w+\mathrm{i}\eta)\right). \tag{6}$$

Substituting the product formula (2) (assuming that it can be used when $\mathrm{Re}\, z = \frac{1}{2}$) into (6) and expanding the logarithms yields

$$N_{\mathrm{osc}}(w) = -\frac{1}{\pi}\,\mathrm{Im}\sum_p\sum_{m=1}^{\infty}\frac{1}{mp^{m/2}}\mathrm{e}^{\mathrm{i}wm\ln(p)}. \tag{7}$$

Therefore the density of zeros along the line $z = \frac{1}{2} - \mathrm{i}w$ can formally be written as

$$\varrho_{\mathrm{osc}}(w) = \frac{\mathrm{d}N_{\mathrm{osc}}}{\mathrm{d}w} = -\frac{1}{\pi}\,\mathrm{Im}\,g(w) \tag{8}$$

with the response function $g(w)$ given by the series

$$g(w) = \mathrm{i}\sum_p\sum_{m=1}^{\infty}\frac{\ln(p)}{p^{m/2}}\mathrm{e}^{\mathrm{i}wm\ln(p)}, \tag{9}$$

which converges only for $\mathrm{Im}\, w > \frac{1}{2}$.

Obviously equation (9) is of the same type as the response function (1), with the entropy barrier $c = \frac{1}{2}$, i.e. equation (9) does not converge on the real axis, where the Riemann zeros are located. The mathematical analogy between the above equation and Gutzwiller's periodic orbit sum

$$\varrho_{\mathrm{osc}}(E) \approx -\frac{1}{\pi}\,\mathrm{Im}\sum_{\mathrm{po}}\mathcal{A}_{\mathrm{po}}\mathrm{e}^{\mathrm{i}S_{\mathrm{po}}}, \tag{10}$$

with $\mathcal{A}_{\mathrm{po}}$ the amplitudes and S_{po} the classical actions (including phase information) of the periodic orbit contributions, was already pointed out by Berry [3, 4]. For the Riemann zeta function the primitive periodic orbits have to be identified with the primes p, and the integer m formally counts the 'repetitions' of orbits. The 'amplitudes' and 'actions' are then given by

$$\mathcal{A}_{pm} = \mathrm{i}\frac{\ln(p)}{p^{m/2}}, \tag{11}$$

$$S_{pm} = mw\ln(p). \tag{12}$$

Both equation (8) for the Riemann zeros and—for most classically chaotic physical systems—the periodic orbit sum (10) do not converge. In particular, zeros of the zeta function, or semiclassical eigenstates, cannot be obtained directly using these expressions. The problem is to find the analytic continuation of these equations to the region where the Riemann zeros or, for physical systems, the eigenenergies and resonances, are located. Equation (9) is the starting point for our introduction and discussion of the harmonic inversion technique for the example of the Riemann zeta function. The generalization of the method to periodic orbit quantization (equation (10)) in section 5 will be straightforward.

Although equation (9) is the starting point for the harmonic inversion method, for completeness we quote the Riemann–Siegel formula, which is the most efficient approach to computing Riemann zeros. For the Riemann zeta function it follows from a functional equation [15] that the function

$$Z(w) = \exp\{-\mathrm{i}[\arg\Gamma(\tfrac{1}{4} + \tfrac{1}{2}\mathrm{i}w) - \tfrac{1}{2}w\ln\pi]\}\zeta(\tfrac{1}{2} - \mathrm{i}w) \tag{13}$$

is real, and even for real w. The asymptotic representation of $Z(w)$ for large w,

$$Z(w) = -2\sum_{n=1}^{\mathrm{Int}[\sqrt{w/2\pi}]} \frac{\cos\{\pi\overline{N}(w) - w\ln n\}}{n^{1/2}} - (-1)^{\mathrm{Int}[\sqrt{w/2\pi}]}\left(\frac{2\pi}{w}\right)^{\frac{1}{4}} \frac{\cos(2\pi(t^2 - t - \frac{1}{16}))}{\cos(2\pi t)} + \cdots, \tag{14}$$

with $t = \sqrt{w/2\pi} - \mathrm{Int}[\sqrt{w/2\pi}]$ is known as the Riemann–Siegel formula and has been employed (with several more correction terms) in effective methods for computing Riemann zeros [17]. Note that the principal sum in (14) has discontinuities at integer positions of $\sqrt{w/2\pi}$, and therefore the Riemann zeros obtained from the principal sum are correct only to about 1–15% of the mean spacing between the zeros. The higher-order corrections to the principal Riemann–Siegel sum remove, one by one, the discontinuities in successive derivatives of $Z(w)$ at the truncation points and are thus essential to obtaining accurate numerical results. An alternative method for improving the asymptotic representation of $Z(w)$ by smoothing the cut-offs with an error function and adding higher-order correction terms is presented in [6].

An analogue of the functional equation for bound and ergodic dynamical systems has been used as the starting point to develop a 'rule for quantizing chaos' via a 'Riemann–Siegel type formula' [4–6]. This method is very efficient as it requires the least number of periodic orbits, but unfortunately it is restricted to ergodic systems on principle reasons, and cannot be generalized either to systems with regular or mixed classical dynamics or to open systems.

By contrast, the method of harmonic inversion does not have these restrictions. We will demonstrate that Riemann zeros can be obtained directly from the 'ingredients' of the non-convergent response function (9), i.e. the set of values A_{pm} and S_{pm}, thus avoiding the use of the functional equation, the Riemann–Siegel formula, the mean staircase function (5), or any other special property of the zeta function. The comparison of results in section 4 will show that the accuracy of our method goes far beyond the Riemann–Siegel formula (14) without higher-order correction terms. The main aim of this paper is to demonstrate that because of the formal equivalence between equations (8) and (10) our method can then be applied to periodic orbit quantization of dynamical systems [20] without any modification.

2.2. The ansatz for the Riemann zeros

To find the analytic continuation of equation (9) in the region $\mathrm{Im}\ w < \frac{1}{2}$ we essentially wish to fit $g(w)$ to its exact functional form,

$$g_{\mathrm{ex}}(w) = \sum_k \frac{d_k}{w - w_k + \mathrm{i}\epsilon}, \tag{15}$$

arising from the definition of the Riemann staircase (4). The 'multiplicities' d_k in equation (15) are formally fitting parameters, which here all should be equal to 1.

It is hard to directly adjust the non-convergent (on the real axis) series $g(w)$ to the form of $g_{\rm ex}(w)$. The first step towards the solution of the problem is to carry out the adjustment for the Fourier components of the response function,

$$C(s) = \frac{1}{2\pi}\int_{-\infty}^{+\infty} g(w)\mathrm{e}^{-\mathrm{i}sw}\,\mathrm{d}w = \mathrm{i}\sum_{p}\sum_{m=1}^{\infty}\frac{\ln(p)}{p^{m/2}}\delta(s - m\ln(p)), \tag{16}$$

which after certain regularizations (see below) is a well-behaved function of s. Due to the formal analogy with the results of periodic orbit theory (see equations (11) and (12)), $C(s)$ can be interpreted as the recurrence function for the Riemann zeta function, with the recurrence positions $S_{pm} = m\ln(p)$ and recurrence strengths of periodic orbit returns $A_{pm} = \mathrm{i}\ln(p)p^{-m/2}$. The exact functional form which now should be used to adjust $C(s)$ is given by

$$C_{\rm ex}(s) = \frac{1}{2\pi}\int_{-\infty}^{+\infty} g_{\rm ex}(w)\mathrm{e}^{-\mathrm{i}sw}\,\mathrm{d}w = -\mathrm{i}\sum_{k=1}^{\infty} d_k\mathrm{e}^{-\mathrm{i}w_k s}. \tag{17}$$

$C_{\rm ex}(s)$ is a superposition of sinusoidal functions with frequencies† w_k given by the Riemann zeros and amplitudes $d_k = 1$.

Fitting a signal $C(s)$ to the functional form of equation (17) with, in general, both complex frequencies w_k and amplitudes d_k is known as *harmonic inversion*, with a large variety of applications in various fields [21–25]. The harmonic inversion analysis is especially non-trivial if the number of frequencies in the signal $C(s)$ is large, e.g. more than a 1000. It is additionally complicated by the fact that the conventional way to perform the spectral analysis by studying the Fourier spectrum of $C(s)$ will bring us back to analysing the non-convergent response function $g(w)$ defined in equation (9). Until recently the known techniques of spectral analysis [21] would not be applicable in this case. It is the filter-diagonalization method [22–24] which has turned the harmonic inversion concept into a general and powerful computational tool.

The signal $C(s)$ as defined by equation (16) is not yet suitable for the spectral analysis. The next step is to regularize $C(s)$ by convoluting it with a Gaussian function to obtain the smoothed signal,

$$C_\sigma(s) = \frac{1}{\sqrt{2\pi}\sigma}\int_{-\infty}^{+\infty} C(s')\mathrm{e}^{-(s-s')^2/2\sigma^2}\mathrm{d}s' = \frac{\mathrm{i}}{\sqrt{2\pi}\sigma}\sum_{p}\sum_{m=1}^{\infty}\frac{\ln(p)}{p^{m/2}}\mathrm{e}^{-(s-m\ln(p))^2/2\sigma^2} \tag{18}$$

that has to be adjusted to the functional form of the corresponding convolution of $C_{\rm ex}(s)$. The latter is readily obtained by substituting d_k in equation (17) by the damped amplitudes,

$$d_k \to d_k^{(\sigma)} = d_k\mathrm{e}^{-w_k^2\sigma^2/2}. \tag{19}$$

The regularization (18) can also be interpreted as a cut of an infinite number of high frequencies in the signal which is of fundamental importance for numerically stable harmonic inversion. Note that the convolution with the Gaussian function is no approximation, and the obtained frequencies w_k and amplitudes d_k corrected by equation (19) are still exact, i.e. do not depend on σ. The convolution is therefore not related to the Gaussian smoothing devised for Riemann zeros in [26] and for quantum mechanics in [27], which provides low-resolution spectra only.

Before proceeding further we note that even though the derivation of equation (18) assumed that the zeros w_k are on the real axis, the analytic properties of $C_\sigma(s)$ imply that

† It is convenient to use the word 'frequencies' for w_k referring to the sinusoidal form of $C(s)$. We will also use the word 'poles' in the context of the response function $g(w)$.

its representation by equation (18) includes not only the non-trivial real zeros, but also all the trivial ones, $w_k = -\mathrm{i}(2k + \frac{1}{2})$, $k = 1, 2, \ldots$, which are purely imaginary. The general harmonic inversion procedure described below does not require the frequencies to be real. Both the real and imaginary zeros w_k will be obtained as the eigenvalues of a non-Hermitian generalized eigenvalue problem.

3. Filter-diagonalization method for harmonic inversion

The harmonic inversion problem can be formulated as a nonlinear fit (see, e.g. [21]) of the signal $C(s)$ defined on an equidistant grid,

$$c_n \equiv C(n\tau) = \sum_k d_k \mathrm{e}^{-\mathrm{i}n\tau w_k}, \qquad n = 0, 1, 2, \ldots N, \tag{20}$$

with the set of generally complex variational parameters $\{w_k, d_k\}$. (In this context the discrete Fourier transform scheme would correspond to a linear fit with N amplitudes d_k and fixed real frequencies $w_k = 2\pi k/N\tau$, $k = 1, 2, \ldots N$. The latter implies the so-called 'uncertainty principle', i.e. the resolution, defined by the Fourier grid spacing, Δw, is inversely proportional to the length, $s_{\max} = N\tau$, of the signal $C(s)$.) The 'high-resolution' property associated with equation (20) is due to the fact that there is no restriction for the closeness of the frequencies w_k as they are variational parameters. In [22] it was shown how this nonlinear fitting problem can be recast as a linear algebraic one using the filter-diagonalization procedure. The essential idea is to associate the signal c_n with an autocorrelation function of a suitable dynamical system,

$$c_n = (\Phi_0, \hat{U}^n \Phi_0), \tag{21}$$

where $(\cdot, \cdot)$ defines a complex symmetric inner product (i.e. no complex conjugation). The evolution operator can be defined implicitly by

$$\hat{U} \equiv \mathrm{e}^{-\mathrm{i}\tau\hat{\Omega}} = \sum_{k=1}^{K} \mathrm{e}^{-\mathrm{i}\tau\omega_k} |\Upsilon_k)(\Upsilon_k|, \tag{22}$$

where the set of eigenvectors $\{\Upsilon_k\}$ is associated with an arbitrary orthonormal basis set and the eigenvalues of $\hat{U}$ are $u_k \equiv \mathrm{e}^{-\mathrm{i}\tau\omega_k}$ (or equivalently the eigenvalues of $\hat{\Omega}$ are ω_k). Inserting equation (22) into equation (21) we obtain equation (20) with

$$d_k = (\Upsilon_k, \Phi_0)^2, \tag{23}$$

which also implicitly defines the 'initial state' Φ_0.

This construction establishes an equivalence between the problem of extracting spectral information from the signal with the one of diagonalizing the evolution operator $\hat{U} = \mathrm{e}^{-\mathrm{i}\tau\hat{\Omega}}$ (or the Hamiltonian $\hat{\Omega}$) of the fictitious underlying dynamical system. The filter-diagonalization method is then used for extracting the eigenvalues of the Hamiltonian $\hat{\Omega}$ in any chosen small energy window. Operationally this is done by solving a small generalized eigenvalue problem whose eigenvalues yield the frequencies in a chosen window. The knowledge of the operator $\hat{\Omega}$ itself is not required, as for a properly chosen basis the matrix elements of $\hat{\Omega}$ can be expressed only in terms of c_n. The advantage of the filter-diagonalization procedure is its numerical stability with respect to both the length and complexity (the number and density of the contributing frequencies) of the signal. Here we apply the method of [23] which is an improvement of the filter-diagonalization method of [22] in that it allows us to significantly reduce the required length of the signal by implementing a different Fourier-type basis with an efficient rectangular filter. Such a

basis is defined by choosing a small set of values φ_j in the frequency interval of interest, $\tau\omega_{\min} < \varphi_j < \tau\omega_{\max}$, $j = 1, 2, \ldots, J$, and the maximum order, M, of the Krylov vectors, $\Phi_n = \mathrm{e}^{-\mathrm{i}n\tau\hat{\Omega}}\Phi_0$, used in the Fourier series,

$$\Psi_j \equiv \Psi(\varphi_j) = \sum_{n=0}^{M} \mathrm{e}^{\mathrm{i}n\varphi_j}\Phi_n \equiv \sum_{n=0}^{M} \mathrm{e}^{\mathrm{i}n(\varphi_j - \tau\hat{\Omega})}\Phi_0. \tag{24}$$

It is convenient to introduce the notations,

$$U^{(p)}_{jj'} \equiv U^{(p)}(\varphi_j, \varphi_{j'}) = (\Psi(\varphi_j), \mathrm{e}^{-\mathrm{i}p\tau\hat{\Omega}}\Psi(\varphi_{j'})), \tag{25}$$

for the matrix elements of the operator $\mathrm{e}^{-\mathrm{i}p\tau\hat{\Omega}}$, and $\boldsymbol{U}^{(p)}$, for the corresponding small $J \times J$ complex symmetric matrix. As such $\boldsymbol{U}^{(1)}$ denotes the matrix representation of the operator $\hat{U}$ itself and $\boldsymbol{U}^{(0)}$, the overlap matrix with elements $(\Psi(\varphi_j), \Psi(\varphi_{j'}))$, which is required as the vectors $\Psi(\varphi_j)$ are not generally orthonormal. Now using these definitions we can set up a generalized eigenvalue problem,

$$\boldsymbol{U}^{(p)}\boldsymbol{B}_k = \mathrm{e}^{-\mathrm{i}p\tau\omega_k}\boldsymbol{U}^{(0)}\boldsymbol{B}_k, \tag{26}$$

for the eigenvalues $\mathrm{e}^{-\mathrm{i}p\tau\omega_k}$ of the operator $\mathrm{e}^{-\mathrm{i}p\tau\hat{\Omega}}$. The column vectors $\boldsymbol{B}_k$ with elements B_{jk} define the eigenvectors Υ_k in terms of the basis functions Ψ_j as

$$\Upsilon_k = \sum_{j=1}^{J} B_{jk}\Psi_j, \tag{27}$$

assuming that the Ψ_j's form a locally complete basis.

The matrix elements (25) can be expressed in terms of the signal c_n, the explicit knowledge of the auxiliary objects $\hat{\Omega}$, Υ_k or Φ_0 is not needed. Indeed, insertion of equation (24) into equation (25), use of the symmetry property, $(\Psi, \hat{U}\Phi) = (\hat{U}\Psi, \Phi)$, and the definition of c_n, equation (21), gives after some arithmetics

$$U^{(p)}(\varphi, \varphi') = (\mathrm{e}^{-\mathrm{i}\varphi} - \mathrm{e}^{-\mathrm{i}\varphi'})^{-1}\Bigg[\mathrm{e}^{-\mathrm{i}\varphi}\sum_{n=0}^{M}\mathrm{e}^{\mathrm{i}n\varphi'}c_{n+p} - \mathrm{e}^{-\mathrm{i}\varphi'}\sum_{n=0}^{M}\mathrm{e}^{\mathrm{i}n\varphi}c_{n+p} - \mathrm{e}^{\mathrm{i}M\varphi}$$
$$\times \sum_{n=M+1}^{2M}\mathrm{e}^{\mathrm{i}(n-M-1)\varphi'}c_{n+p} + \mathrm{e}^{\mathrm{i}M\varphi'}\sum_{n=M+1}^{2M}\mathrm{e}^{\mathrm{i}(n-M-1)\varphi}c_{n+p}\Bigg], \qquad \varphi \neq \varphi' \tag{28}$$

$$U^{(p)}(\varphi, \varphi) = \sum_{n=0}^{2M}(M - |M - n| + 1)\mathrm{e}^{\mathrm{i}n\varphi}c_{n+p}.$$

(Note that the evaluation of $\mathrm{U}^{(p)}$ requires knowledge of c_n for $n = p, p+1, \ldots, N = 2M + p$.)

The solution of the generalized eigenvalue problem (26) is usually done by a singular value decomposition of the matrix $\mathrm{U}^{(0)}$. Each value of p yields a set of frequencies w_k and, due to equations (23), (24) and (27), amplitudes,

$$d_k = \left(\sum_{j=1}^{J} B_{jk}\sum_{n=0}^{M} c_n\mathrm{e}^{\mathrm{i}n\varphi_j}\right)^2. \tag{29}$$

Note that equation (29) is a functional of the half-signal $c_n, n = 1, 2, \ldots, M$. Even though in all our applications equation (29) yields very good results, here we present an even better expression for the coefficients d_k (see [24]),

$$d_k = \left[\frac{1}{M+1}\sum_{j=1}^{J} B_{jk}(\Psi(\varphi_j), \Psi(w_k))\right]^2 \equiv \left[\frac{1}{M+1}\sum_{j=1}^{J} B_{jk}U^{(0)}(\varphi_j, w_k)\right]^2 \tag{30}$$

with $U^{(0)}(\varphi_j, w_k)$ defined by equation (28). Equation (30) is a functional of the whole available signal c_n, $n = 0, 1, \ldots, 2M$.

The converged w_k and d_k should not depend on p. This condition allows us to identify spurious or non-converged frequencies by comparing the results with different values of p (e.g. with $p = 1$ and $p = 2$). We can define the simplest error estimate ε as the difference between the frequencies w_k obtained from diagonalizations with $p = 1$ and $p = 2$, i.e.

$$\varepsilon = |w_k^{(p=1)} - w_k^{(p=2)}|. \tag{31}$$

4. Riemann zeros by harmonic inversion

In section 2 we introduced the method for periodic orbit quantization by harmonic inversion for the example of the Riemann zeta function because this model allows a direct check of the precision of our method. In this section we present and discuss the numerical results obtained for the Riemann zeros. We also discuss the amount of periodic orbit input data, namely here the prime numbers, required to obtain converged semiclassical eigenenergies and Riemann zeros, respectively.

4.1. Numerical results

For a numerical demonstration we construct the signal $C_\sigma(s)$ using equations (16) and (18) in the region $s < \ln(10^6) = 13.82$ from the first 78 498 prime numbers and with a Gaussian smoothing width $\sigma = 0.0003$. Parts of the signal are presented in figure 1. Up to $s \approx 8$ the Gaussian approximations to the δ-functions do essentially not overlap (see figure 1(a)) whereas for $s \gg 8$ the mean spacing Δs between successive δ-functions becomes much less than the Gaussian width $\sigma = 0.0003$ and the signal fluctuates around the mean $\overline{C}(s) = \mathrm{i}\mathrm{e}^{s/2}$ (see figure 1(b)). From this signal we were able to calculate about 2600 Riemann zeros to at least 12 digit precision. For the small generalized eigenvalue problem (26) we used matrices with dimension $J < 100$. Some Riemann zeros w_k, the corresponding amplitudes d_k, and the estimated errors ε (see equation (31)) are given in table 1. Within the numerical error the Riemann zeros are real and the amplitudes are consistent with $d_k = 1$ for non-degenerate zeros. To fully appreciate the accuracy of our harmonic inversion technique we note that zeros obtained from the principal sum of the Riemann–Siegel formula (14) deviate by about 1–15% of the mean spacing from the exact zeros. Including the first correction term in (14) the approximations to the first five zeros read $w_1 = 14.137$, $w_2 = 21.024$, $w_3 = 25.018$, $w_4 = 30.428$ and $w_5 = 32.933$, which still significantly deviates from the exact values (see table 1). Considering even higher-order correction terms the results will certainly converge to the exact zeros. However, the generalization of such higher-order corrections to ergodic dynamical systems is a non-trivial task and requires, e.g. the knowledge of the terms in the Weyl series, i.e. the mean staircase function after the constant [6, 29]. The perfect agreement of our results for the w_k with the exact Riemann zeros to full numerical precision is remarkable and clearly demonstrates that harmonic inversion by filter-diagonalization is a very powerful and accurate technique for the analytic continuation and the extraction of poles of a non-convergent series such as equation (1).

A few w_k have been obtained (see table 2) which are definitely not located on the real axis. Except for the first at $w = \mathrm{i}/2$ they can be identified with the trivial real zeros of the zeta function at $z = -2n$; $n = 1, 2, \ldots$. In contrast to the non-trivial zeros with real w_k, the numerical accuracy for the trivial zeros decreases rapidly with increasing n. The trivial zeros $w_n = -\mathrm{i}(2n + \frac{1}{2})$ are the analogue of resonances in open physical systems with

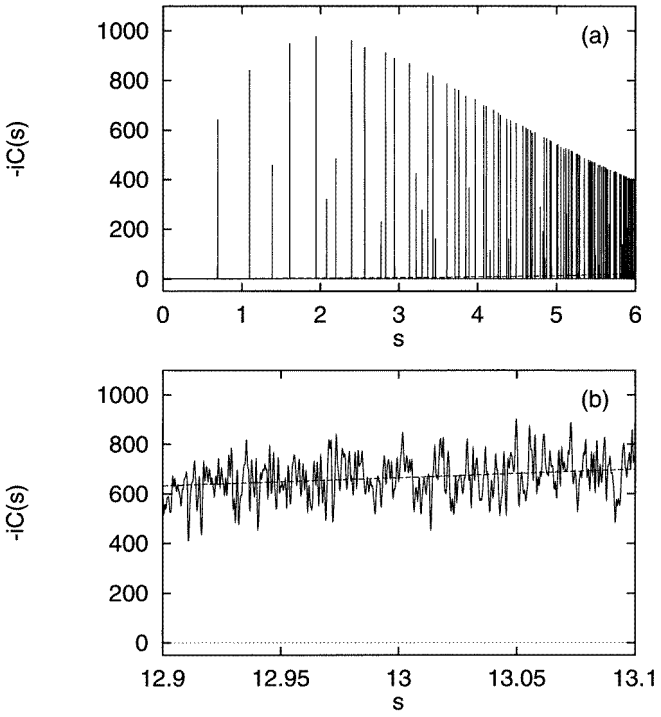

Figure 1. 'Recurrence' function $-\mathrm{i}C_\sigma(s)$ for the Riemann zeros which has been analysed by harmonic inversion. (*a*) Range $0 \leqslant s \leqslant 6$. (*b*) Short range around $s = 13$. The δ-functions have been convoluted by a Gaussian function with width $\sigma = 0.0003$. Broken line: smooth background $\overline{C}(s) = \mathrm{i}\mathrm{e}^{s/2}$ resulting from the pole of the zeta function.

widths increasing with n. The fact that the trivial Riemann zeros are obtained emphasizes the general applicability of our method and demonstrates that periodic orbit quantization by harmonic inversion can be applied not only to closed but to open systems as well. The decrease of the numerical accuracy for very broad resonances is a natural numerical consequence of the harmonic inversion procedure [23, 24].

The value $w = \mathrm{i}/2$ in table 2 is special because in this case the amplitude is negative, i.e. $d_k = -1$. Writing the zeta function in the form [16]

$$\zeta(\tfrac{1}{2} - \mathrm{i}w) = C \prod_k (w - w_k)^{d_k} A(w, w_k) \tag{32}$$

where C is a constant and A a regularizing function which ensures convergence of the product, integer values d_k are the multiplicities of *zeros*. Therefore it is reasonable to relate negative integer values with the multiplicities of *poles*. In fact, $\zeta(z)$ has a simple pole at $z = \frac{1}{2} - \mathrm{i}w = 1$ consistent with $w = \mathrm{i}/2$ in table 2.

4.2. Required signal length

We have calculated Riemann zeros by harmonic inversion of the signal $C_\sigma(s)$ (equation (18)) which uses prime numbers as input. The question arises as to what the requirements are on the signal $C_\sigma(s)$ and, in particular, what the required signal length is. In other words, how many Riemann zeros (or semiclassical eigenenergies) can be converged for a given set of

Table 1. Non-trivial zeros w_k, multiplicities d_k and error estimate ε for the Riemann zeta function.

k	Re w_k	Im w_k	Re d_k	Im d_k	ε
1	14.134 725 14	4.05E-12	1.000 000 11	−5.07E-08	3.90E-13
2	21.022 039 64	−2.23E-12	1.000 000 14	1.62E-07	9.80E-13
3	25.010 857 58	1.66E-11	0.999 999 75	−2.64E-07	5.20E-12
4	30.424 876 13	−6.88E-11	0.999 999 81	−1.65E-07	1.90E-12
5	32.935 061 59	7.62E-11	1.000 000 20	5.94E-08	7.10E-13
6	37.586 178 16	1.46E-10	1.000 000 34	5.13E-07	1.00E-12
7	40.918 719 01	−3.14E-10	0.999 998 56	1.60E-06	4.90E-11
8	43.327 073 28	1.67E-11	1.000 000 08	3.29E-07	1.90E-12
9	48.005 150 88	4.35E-11	0.999 999 75	−1.35E-07	1.40E-12
10	49.773 832 48	7.02E-11	1.000 002 54	−4.59E-07	1.10E-10
11	52.970 321 48	1.92E-10	1.000 001 22	7.31E-07	6.00E-11
12	56.446 247 70	−1.30E-10	0.999 999 93	4.51E-07	5.50E-12
13	59.347 044 00	5.40E-11	0.999 999 54	2.34E-06	2.30E-10
14	60.831 778 52	−3.94E-10	1.000 000 14	1.11E-06	3.00E-11
15	65.112 544 06	−4.98E-09	0.999 980 10	−8.30E-06	2.70E-08
...	...	...	...	...	...
2551	3083.361 357 98	8.43E-10	0.999 999 23	3.45E-07	1.50E-11
2552	3084.838 451 50	2.72E-09	1.000 000 57	−2.86E-06	1.80E-10
2553	3085.377 268 98	−1.37E-08	0.999 995 76	−2.88E-06	5.50E-10
2554	3085.965 522 25	6.39E-09	0.999 996 67	1.50E-06	2.80E-10
2555	3087.018 815 35	3.46E-11	0.999 998 45	−3.63E-07	5.20E-11
2556	3088.083 437 03	−3.89E-10	0.999 999 31	−8.44E-07	2.40E-11
2557	3089.222 308 94	−3.31E-10	1.000 000 17	−9.21E-07	1.80E-11
2558	3090.282 194 90	2.97E-10	1.000 000 69	−7.17E-07	2.10E-11
2559	3091.154 469 69	1.10E-09	1.000 000 52	−6.59E-07	1.50E-11
2560	3092.687 667 04	2.25E-09	1.000 000 33	1.45E-06	5.20E-11
2561	3093.185 445 71	−2.33E-09	1.000 001 68	−1.50E-07	6.40E-11
2562	3094.833 068 42	2.07E-08	0.999 996 47	2.63E-06	4.20E-10
2563	3095.132 031 22	−1.79E-08	1.000 004 59	1.70E-06	5.20E-10
2564	3096.515 485 51	5.15E-09	0.999 998 68	2.74E-06	2.20E-10
2565	3097.342 606 55	7.75E-09	0.999 999 18	5.12E-06	6.00E-10
2566	3098.038 354 98	−2.14E-08	1.000 002 96	4.34E-06	6.20E-10

Table 2. Trivial zeros and pole of the Riemann zeta function.

Re w_k	Im w_k	Re d_k	Im d_k	ε
0.000 000 00	0.500 000 00	−1.000 000 02	−4.26E-08	1.80E-14
−0.000 000 60	−2.499 999 41	0.999 924 87	−3.66E-05	1.80E-07
−0.001 299 15	−4.499 879 11	1.000 699 39	−3.25E-03	4.40E-05
−0.097 611 73	−6.532 860 64	1.071 414 45	−1.49E-01	1.70E-03

prime numbers (or periodic orbits, respectively)? The answer can be directly obtained from the requirements on the harmonic inversion technique. In general, the required signal length $s_{\max}$ for harmonic inversion is related to the average density of frequencies $\overline{\varrho}(w)$ by [24]

$$s_{\max} \approx 4\pi\overline{\varrho}(w). \tag{33}$$

From equation (33) the required number of primes (or periodic orbits) can be directly estimated as {# primes $p|\ln p < s_{\max}$} or {number of periodic orbits $|s_{\mathrm{po}} < s_{\max}$}. For the special example of the Riemann zeta function the required number of primes to have a

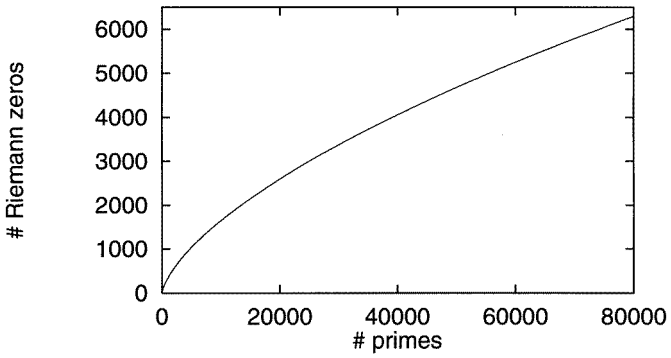

Figure 2. Estimated number of converged zeros of the Riemann zeta function, which can be obtained by harmonic inversion for a given number of primes p.

given number of Riemann zeros converged can be estimated analytically. With the average density of Riemann zeros derived from (5),

$$\overline{\varrho}(w) = \frac{\mathrm{d}\overline{N}}{\mathrm{d}w} = \frac{1}{2\pi} \ln\left(\frac{w}{2\pi}\right) \tag{34}$$

we obtain

$$s_{\max} = \ln(p_{\max}) = 2\ln\left(\frac{w}{2\pi}\right) \Rightarrow p_{\max} = \left(\frac{w}{2\pi}\right)^2. \tag{35}$$

The number of primes with $p < p_{\max}$ can be estimated from the prime number theorem

$$\pi(p_{\max}) \sim \frac{p_{\max}}{\ln(p_{\max})} = \frac{(w/2\pi)^2}{2\ln(w/2\pi)}. \tag{36}$$

On the other hand the number of Riemann zeros as a function of w is given by equation (5). The estimated number of Riemann zeros which can be obtained by harmonic inversion from a given set of primes is presented in figure 2. For example, about 80 zeros ($w < 200$) can be extracted from the short signal $C_\sigma(s)$ with $s_{\max} = \ln(1000) = 6.91$ (168 prime numbers) in agreement with the estimates given above. Obviously, in the special case of the Riemann zeta function the efficiency of our method cannot compete with that of the Riemann–Siegel formula method (14) where the number of terms is given by $n_{\max} = \mathrm{Int}[\sqrt{w/2\pi}]$ and, e.g. five terms in equation (14) would be sufficient to calculate good approximations to the Riemann zeros in the region $w < 200$. Our primary intention is to introduce harmonic inversion by way of example of the zeros of the Riemann zeta function as a *general* tool for periodic orbit quantization, and not to use it as an alternative method for solving the problem of finding most efficiently zeros of the Riemann zeta function.

A functional equation can only be invoked for the semiclassical quantization of *bound* and *ergodic* systems. In this case the required number of periodic orbits can be estimated from the condition $s_{\max} \approx \pi\overline{\varrho}(w)$ [4–6], which differs by a factor of 4 from the required signal length (33) for harmonic inversion. Periodic orbit quantization by harmonic inversion will be of particular advantage in situations where special properties such as a functional equation cannot be invoked, e.g. for bound systems with non-ergodic, i.e. regular or mixed classical dynamics, and for open (scattering) systems.

4.3. A remark on the Riemann hypotheses

We conclude this section with a remark on the famous Riemann hypotheses mentioned in section 2.1. Applying our method of harmonic inversion to the signal $C_\sigma(s)$ (equation (18)) the Riemann hypotheses for the *zeros* of the zeta function, $\zeta(z = \frac{1}{2} - \mathrm{i}w_k) = 0$, is directly related to an equivalent statement for the *eigenvalues* $\mathrm{e}^{-\mathrm{i}\tau w_k}$ of the operator $\mathrm{e}^{-\mathrm{i}\tau\hat{\Omega}}$, i.e. the generalized eigenvalue problem (26). Speculations that the operator $\hat{\Omega}$ can be regarded as the Hamiltonian of a quantum-mechanical system have been presented by Berry [3]. Unfortunately, $\hat{\Omega}$ is not known as it is only defined implicitly by way of its matrix representation (28), which is a linear functional of the signal (18). However, the very fact that the Riemann zeros are obtained as eigenvalues of some matrix with analytically known coefficients is already intriguing.

5. Periodic orbit quantization

As mentioned in section 2 the basic equation (9) used for the calculation of Riemann zeros has the same mathematical form as Gutzwiller's semiclassical trace formula. Both series, equation (9) and the periodic orbit sum (10), suffer from similar convergence problems in that they are absolutely convergent only in the complex half-plane outside the region where the Riemann zeros, or quantum eigenvalues, respectively, are located. As a consequence, in a direct summation of periodic orbit contributions smoothing techniques must be applied resulting in low-resolution spectra for the density of states [27, 30]. To extract individual eigenstates the semiclassical trace formula has to be analytically continued to the region of the quantum poles. Here dynamical zeta functions have turned out to be of particular interest.

For *bound* and *ergodic* systems one technique is to apply an approximate functional equation and generalize the Riemann–Siegel formula (14) to dynamical zeta functions [4–6]. The Riemann–Siegel-type formula has been applied, e.g. for the semiclassical quantization of the hyperbola billiard [28, 29]. For bound ergodic systems alternative semiclassical quantization conditions based on a semiclassical representation of the spectral staircase $\mathcal{N}(E) = \sum_n \Theta(E - E_n)$ [7, 8] and derived from a quantum version of a classical Poincaré map [9] have also been discussed.

These quantization techniques cannot be applied to *open* systems. However, if a symbolic dynamics for the system exists, i.e. if the periodic orbits can be classified with the help of a complete symbolic code, the dynamical zeta function, given as an infinite Euler product over entries from classical periodic orbits can be expanded in terms of the cycle length of the orbits [10, 11]. The *cycle expansion* series is rapidly convergent if the contributions of long orbits are approximately shadowed by contributions of short orbits. The cycle expansion technique has been applied, e.g. to the three-disk scattering system [10, 12, 13], the three-body Coulomb system [31, 32], and to the hydrogen atom in a magnetic field [33]. A combination of the cycle-expansion method with a functional equation has been applied to bound systems in [14, 34]. However, the existence of a complete symbolic dynamics is more the exception than the rule, and the cycle expansion cannot be applied, in particular for systems with mixed regular–chaotic classical dynamics.

In this section we apply the same technique that we used for the calculation of Riemann zeros, to the calculation of semiclassical eigenenergies and resonances of physical systems by harmonic inversion of Gutzwiller's periodic orbit sum for the propagator. The method only requires the knowledge of all orbits up to a sufficiently long but finite period and does not rely on either an approximate semiclassical functional equation, nor does it depend

on the existence of a symbolic code for the orbits. The method will therefore allow the investigation of a large variety of systems with an underlying chaotic, mixed, or even regular classical dynamics. The derivation of an expression for the recurrence function to be harmonically inverted is analogous to that in section 2.2.

5.1. Semiclassical density of states

Following Gutzwiller [1, 2] the semiclassical response function for chaotic systems is given by

$$g^{\mathrm{sc}}(E) = g_0^{\mathrm{sc}}(E) + \sum_{\mathrm{po}} \mathcal{A}_{\mathrm{po}} \mathrm{e}^{\mathrm{i}S_{\mathrm{po}}}, \tag{37}$$

where $g_0^{\mathrm{sc}}(E)$ is a smooth function and the S_{po} and $\mathcal{A}_{\mathrm{po}}$ are the classical actions and weights (including phase information given by the Maslov index) of periodic orbit contributions. Equation (37) is also valid for integrable [35] and near-integrable [36, 37] systems but with different expressions for the amplitudes $\mathcal{A}_{\mathrm{po}}$. It should also be possible to include complex 'ghost' orbits [38, 39] and uniform semiclassical approximations [40, 41] close to bifurcations of periodic orbits in the semiclassical response function (37). The eigenenergies and resonances are the poles of the response function but, unfortunately, its semiclassical approximation (37) does not converge in the region of the poles, whence the problem is the analytic continuation of $g^{\mathrm{sc}}(E)$ to this region.

In the following we make the (weak) assumption that the classical system has a scaling property, i.e. the shape of periodic orbits does not depend on the scaling parameter, w, and the classical action scales as

$$S_{\mathrm{po}} = w s_{\mathrm{po}}. \tag{38}$$

Examples of scaling systems are billiards [10, 42], Hamiltonians with homogeneous potentials [43, 44], Coulomb systems [32], or the hydrogen atom in external magnetic and electric fields [45, 33]. Equation (38) can even be applied for non-scaling, e.g. molecular systems if a generalized scaling parameter $w \equiv \overline{h}_{\mathrm{eff}}^{-1}$ is introduced as a new dynamical variable [46]. Quantization yields bound states or resonances, w_k, for the scaling parameter. In scaling systems the semiclassical response function $g^{\mathrm{sc}}(w)$ can be Fourier transformed easily to obtain the semiclassical trace of the propagator

$$C^{\mathrm{sc}}(s) = \frac{1}{2\pi} \int_{-\infty}^{+\infty} g^{\mathrm{sc}}(w) \mathrm{e}^{-\mathrm{i}sw} \, \mathrm{d}w = \sum_{\mathrm{po}} \mathcal{A}_{\mathrm{po}} \delta(s - s_{\mathrm{po}}). \tag{39}$$

The signal $C^{\mathrm{sc}}(s)$ has δ-peaks at the positions of the classical periods (scaled actions) $s = s_{\mathrm{po}}$ of periodic orbits and with peak heights (recurrence strengths) $\mathcal{A}_{\mathrm{po}}$, i.e. $C^{\mathrm{sc}}(s)$ is Gutzwiller's periodic orbit recurrence function. Consider now the quantum-mechanical counterparts of $g^{\mathrm{sc}}(w)$ and $C^{\mathrm{sc}}(w)$ taken as the sums over the poles w_k of the Green's function,

$$g^{\mathrm{qm}}(w) = \sum_k \frac{d_k}{w - w_k + \mathrm{i}\epsilon}, \tag{40}$$

$$C^{\mathrm{qm}}(s) = \frac{1}{2\pi} \int_{-\infty}^{+\infty} g^{\mathrm{qm}}(w) \mathrm{e}^{-\mathrm{i}sw} \, \mathrm{d}w = -\mathrm{i} \sum_k d_k \mathrm{e}^{-\mathrm{i}w_k s}, \tag{41}$$

with d_k being the multiplicities of resonances, i.e. $d_k = 1$ for non-degenerate states. In analogy with the calculation of Riemann zeros from equation (18) the frequencies, w_k,

and amplitudes, d_k, can now be extracted by harmonic inversion of the signal $C^{\mathrm{sc}}(s)$ after convoluting it with a Gaussian function, i.e.

$$C^{\mathrm{sc}}_{\sigma}(s) = \frac{1}{\sqrt{2\pi}\sigma} \sum_{\mathrm{po}} \mathcal{A}_{\mathrm{po}} \mathrm{e}^{(s-s_{\mathrm{po}})^2/2\sigma^2}. \tag{42}$$

By adjusting $C^{\mathrm{sc}}_{\sigma}(s)$ to the functional form of equation (41), the frequencies, w_k, can be interpreted as the semiclassical approximation to the poles of the Green's function in (40). Note that the harmonic inversion method described in section 3 also allows studying signals with complex frequencies w_k. For open systems the complex frequencies can be interpreted as semiclassical resonances. Note also that the w_k in general differ from the exact quantum eigenvalues because Gutzwiller's trace formula (37) is an approximation, correct only to first order in $\overline{h}$. Therefore the diagonalization of small matrices in (26) does not imply that the results of periodic orbit quantization are more 'quantum' in any sense than those obtained, e.g. from a cycle expansion [10, 11]. The eigenvalues are solutions of nonlinear equations and the diagonalization is equivalent to the search of zeros of the dynamical zeta function in the cycle expansion technique. Numerical calculation of the zeros is also a nonlinear problem and, in contrast to the matrix diagonalization, might encounter a problem of missing roots.

5.2. Semiclassical matrix elements

The procedure described above can be generalized in a straightforward manner to the calculation of semiclassical diagonal matrix elements $\langle\psi_k|\hat{A}|\psi_k\rangle$ of a smooth Hermitian operator $\hat{A}$. In this case we start from the quantum-mechanical trace formula [47]

$$g^{\mathrm{qm}}_A(w) = \mathrm{tr}\, G^+\hat{A} = \sum_k \frac{\langle\psi_k|\hat{A}|\psi_k\rangle}{w - w_k + \mathrm{i}\epsilon}, \tag{43}$$

which has the same functional form as (40), but with $d_k = \langle\psi_k|\hat{A}|\psi_k\rangle$ instead of $d_k = 1$. For the quantum response function $g^{\mathrm{qm}}_A(w)$ (equation (43)) a semiclassical approximation has been derived in [47], which has the same form as Gutzwiller's trace formula (37) but with amplitudes

$$\mathcal{A}_{\mathrm{po}} = -\mathrm{i}\frac{A_p \mathrm{e}^{-\mathrm{i}\frac{\pi}{2}\mu_{\mathrm{po}}}}{\sqrt{|\det(M_{\mathrm{po}} - I)|}} \tag{44}$$

where M_{po} is the monodromy matrix and μ_{po} the Maslov index of the periodic orbit, and

$$A_p = \int_0^{S_p} A(\boldsymbol{q}(s), \boldsymbol{p}(s))\, \mathrm{d}s \tag{45}$$

is the classical average of the observable A over *one* period S_p of the *primitive* periodic orbit. Note that $\boldsymbol{q}(s)$ and $\boldsymbol{p}(s)$ are functions of the classical action instead of time for scaling systems [48]. Gutzwiller's trace formula for the density of states is obtained with $\hat{A}$ being the identity operator, i.e. $A_p = S_p$. When the semiclassical signal $C^{\mathrm{sc}}(s)$ (equation (39)) with amplitudes $\mathcal{A}_{\mathrm{po}}$ given by equations (44) and 45 is analysed with the method of harmonic inversion the frequencies and amplitudes obtained are the semiclassical approximations to the eigenvalues w_k and matrix elements $d_k = \langle\psi_k|\hat{A}|\psi_k\rangle$, respectively.

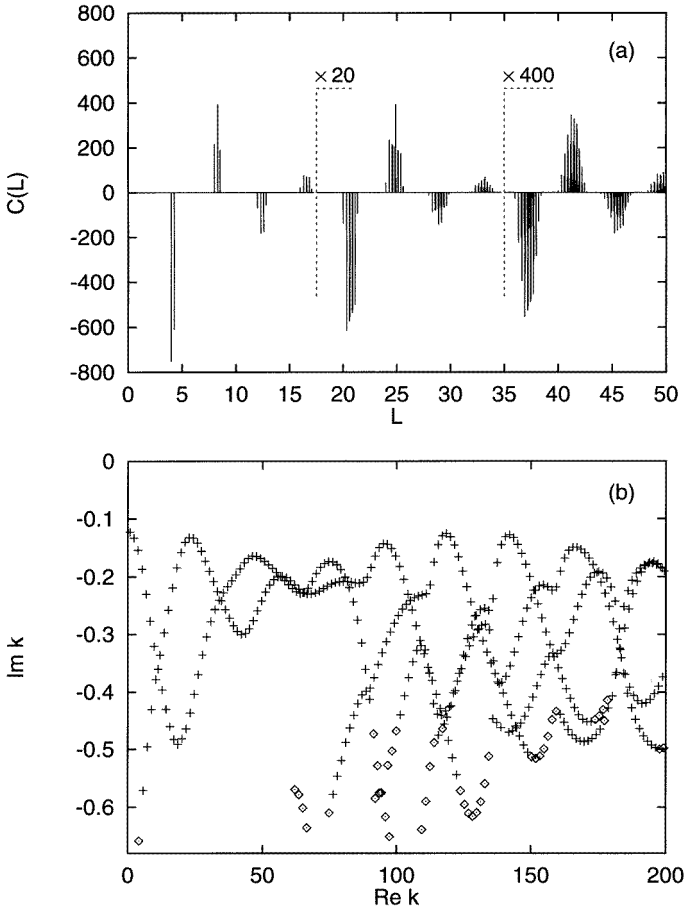

Figure 3. Three-disk scattering system (A_1 subspace) with $R = 1$, $d = 6$. (a) Periodic orbit recurrence function, $C(L)$. The signal has been convoluted with a Gaussian function of width $\sigma = 0.0015$. (b) Semiclassical resonances. The resonance positions marked by diamonds might be less accurate (see text).

6. The three-disk scattering system

Let us consider a billiard system consisting of three identical hard disks with unit radii, $R = 1$, displaced from each other by the same distance d. This simple, albeit non-trivial, scattering system has served as a model for periodic orbit quantization in many investigations in recent years [49, 10, 12, 13]. After symmetry reduction the periodic orbits can be classified by a binary symbolic code [10]. For $d > 2.1$ there is a one-to-one identity between the periodic orbits and the symbolic code, whereas for $d < 2.1$ pruning of orbits sets in. For $d = 6$ semiclassical resonances were calculated by application of the cycle expansion technique including all periodic orbits up to cycle length $n = 13$ [13]. In order to demonstrate the usefulness of the harmonic inversion technique we first apply it to the case $R : d = 1 : 6$ studied before. Note that the ratio corresponds to the very favourable regime for the cycle expansion (see below). In billiards the scaled action s is given by the length L of orbits ($s = L$) and the quantized parameter is the absolute value of the wavevector $k = |\boldsymbol{k}| = \sqrt{2mE}/\hbar$. Figure 3($a$) shows the periodic orbit recurrence

Table 3. Semiclassical resonances, multiplicities and error estimates for the three-disk scattering problem (A_1 subspace) with $R = 1$, $d = 6$. The marked resonances are plotted as diamonds in figure 3(*b*).

Re k	Im k	Re d	Im d	ε
0.758 313 90	−0.122 822 20	0.999 999 98	−0.000 000 01	2.84E-12
2.274 278 57	−0.133 058 73	1.000 000 00	0.000 000 00	2.71E-14
3.787 876 78	−0.154 127 39	1.000 000 01	0.000 000 00	1.11E-13
◊4.145 689 80	−0.658 539 72	0.942 612 84	−0.057 822 00	1.79E-06
5.296 067 78	−0.186 787 31	1.000 000 00	0.000 000 04	2.63E-12
5.681 497 60	−0.571 372 10	0.995 127 63	−0.017 390 98	5.34E-07
6.793 636 53	−0.229 922 12	0.999 999 94	0.000 000 18	1.54E-11
7.224 057 97	−0.495 424 27	1.000 920 01	−0.004 619 67	4.02E-07
8.276 390 62	−0.277 080 51	1.000 000 64	−0.000 000 07	3.47E-11
8.779 213 37	−0.430 256 11	0.999 000 81	0.001 205 44	1.00E-07
9.747 632 87	−0.320 817 04	0.999 999 86	0.000 000 49	6.32E-12
10.344 225 66	−0.378 198 84	1.000 001 89	0.000 011 09	3.89E-10
11.213 477 81	−0.359 963 94	1.000 001 80	−0.000 004 02	3.87E-10
11.913 449 55	−0.335 734 55	0.999 998 31	−0.000 000 66	2.50E-10
12.677 531 89	−0.396 115 36	0.999 978 60	−0.000 007 36	3.04E-09
13.482 648 92	−0.296 947 75	1.000 000 38	−0.000 000 54	6.90E-11
14.142 413 58	−0.430 060 40	1.000 078 02	0.000 081 49	2.54E-08
...	...	...	...	...
125.730 609 52	−0.338 687 44	1.000 353 74	0.000 899 53	1.76E-08
126.168 127 80	−0.217 265 68	0.999 975 32	0.000 005 23	6.34E-10
126.570 000 32	−0.307 179 94	0.999 698 30	−0.000 287 69	6.87E-09
◊126.898 633 30	−0.610 583 35	1.248 549 08	−0.162 904 32	3.18E-06
127.217 596 81	−0.320 102 87	1.000 427 52	0.000 452 32	1.30E-08
127.683 086 51	−0.243 413 98	0.999 936 10	−0.000 002 36	2.13E-09
128.121 160 88	−0.283 896 37	1.000 101 75	−0.000 222 29	4.95E-09
◊128.411 372 17	−0.615 774 14	1.324 225 38	−0.115 650 68	4.11E-06
128.703 340 65	−0.304 426 55	1.000 395 70	0.000 113 10	8.78E-09
129.197 329 46	−0.267 888 59	0.999 876 56	−0.000 044 93	5.25E-09
129.673 196 99	−0.267 178 42	1.000 178 17	0.000 026 64	4.62E-09
◊129.929 272 07	−0.609 183 15	1.333 229 88	−0.021 703 82	4.76E-06
130.187 962 23	−0.292 235 40	1.000 283 13	−0.000 127 43	6.65E-09
130.710 980 79	−0.290 452 41	0.999 832 13	−0.000 126 09	8.19E-09
131.227 178 21	−0.257 364 73	1.000 000 71	0.000 173 24	5.54E-09
◊131.448 892 08	−0.590 543 85	1.266 103 20	0.069 730 01	4.99E-06
131.671 395 81	−0.284 297 11	1.000 100 65	−0.000 276 24	6.60E-09

function, i.e. the trace of the semiclassical propagator $C^{\mathrm{sc}}(L)$. The groups with oscillating sign belong to periodic orbits with adjacent cycle lengths. To obtain a smooth function on an equidistant grid, which is required for the harmonic inversion method, the δ-functions in (39) have been convoluted with a Gaussian function of width $\sigma = 0.0015$. As explained in section 2, this does not change the underlying spectrum. The results of the harmonic inversion analysis of this signal are presented in figure 3(*b*) and table 3. The crosses in figure 3(*b*) represent semiclassical poles, for which the amplitudes d_k are very close to 1, mostly within 1%. Because the amplitudes converge much slower than the frequencies these resonance positions can be assumed to be very accurate within the semiclassical approximation. In fact, a perfect agreement to many significant figures is achieved for these poles with the results obtained by cycle expansion [13], and this agreement confirms that the results in figure 3(*b*) and table 3 are the true semiclassical resonances, i.e. deviations from

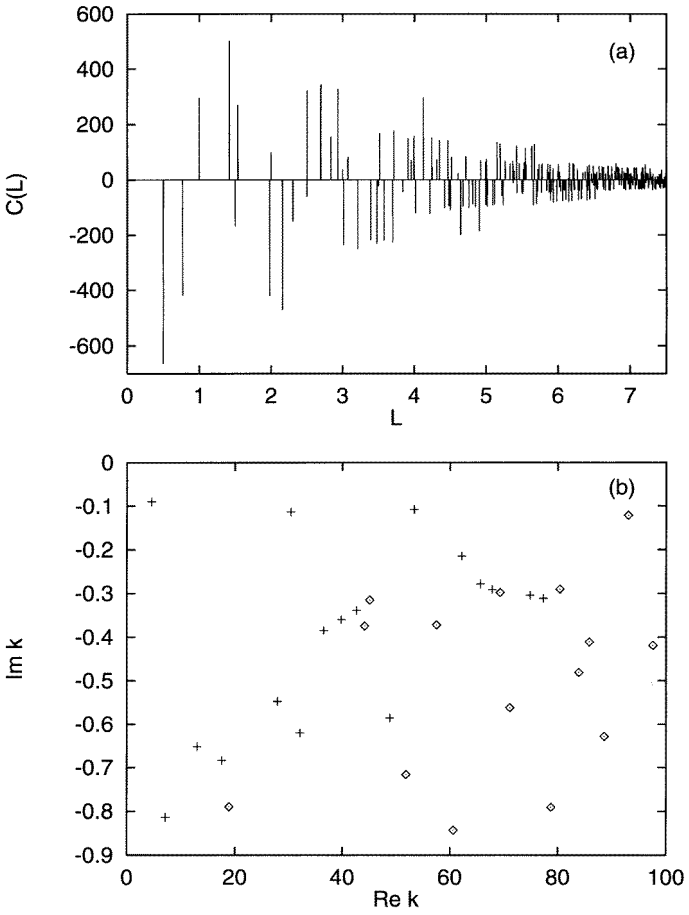

Figure 4. Three-disk scattering system (A_1 subspace) with $R = 1$, $d = 2.5$. (a) Periodic orbit recurrence function, $C(L)$. The signal has been convoluted with a Gaussian function of width $\sigma = 0.0003$. (b) Semiclassical resonances. The resonance positions marked by diamonds might be less accurate (see text).

the exact quantum poles are solely due to the semiclassical approximation in Gutzwiller's trace formula.

For some broad resonances marked by diamonds in figure 3(b) and table 3 the d_k deviate strongly from 1, within 5% to maximal 50%. It is not clear whether these strong deviations are due to numerical effects, such as convergence problems caused by too short a signal, or if they are a direct consequence of the semiclassical approximation. Of course, in the exact expression (41) all multiplicities d_k are 1, but there is no proof that this is still true within the semiclassical approximation. However, for the lowest k eigenvalues (see, e.g. the first three resonances in table 3), where the agreement with the exact resonance energies is worst [13] $d_k = 1$ still holds, indicating that there is no $\overline{h}$-dependence for the multiplicities.

The cycle expansion technique is based on the idea that the contributions of long periodic orbits are shadowed by those of short orbits. For the three-disk scattering system this is ideally fulfilled in the limit of a large ratio $d/R \gg 2$. This is no longer true for short distances between the disks and hence the convergence of the conventional cycle expansion

Table 4. Semiclassical resonances, multiplicities and error estimates for the three-disk scattering problem (A_1 subspace) with $R = 1$, $d = 2.5$ obtained from the signal $C(L)$ with $L < 7.5$ in figure 4(a). The marked resonances are plotted as diamonds in figure 4(b).

Re k	Im k	Re d	Im d	ε
4.581 222 47	−0.089 991 48	1.000 004 17	0.001 202 03	6.97E-08
7.142 669 60	−0.813 910 29	1.018 349 65	−0.008 231 13	3.51E-06
12.999 511 05	−0.651 664 27	1.000 420 48	−0.000 568 55	1.31E-06
17.563 226 89	−0.683 569 06	0.984 597 03	−0.030 607 11	2.28E-05
◊18.910 242 31	−0.789 568 16	1.034 978 67	−0.072 093 60	6.09E-05
27.887 928 68	−0.547 372 25	1.023 534 31	0.003 931 94	2.30E-05
30.388 710 17	−0.113 673 91	1.001 219 48	0.007 471 17	2.68E-06
32.098 373 18	−0.620 041 77	0.990 022 66	0.013 682 55	3.50E-05
36.507 210 98	−0.384 893 03	1.001 362 14	0.010 155 58	9.58E-06
39.811 547 07	−0.359 778 01	1.007 780 64	−0.005 965 26	7.00E-05
42.656 969 84	−0.339 108 75	0.953 168 03	0.029 423 69	1.81E-05
◊44.155 611 23	−0.374 423 67	0.703 667 81	−0.279 272 32	9.13E-05
◊45.096 704 13	−0.315 063 05	0.772 862 61	0.105 648 55	2.54E-05
48.843 672 80	−0.585 475 64	0.972 051 65	0.018 328 79	3.83E-06
◊51.855 397 38	−0.715 821 11	1.059 988 79	−0.227 548 26	7.06E-05
53.368 848 96	−0.107 799 98	1.039 031 58	−0.031 956 38	7.48E-06
◊57.526 232 96	−0.372 003 26	0.544 802 46	0.049 479 34	6.95E-05
◊60.632 586 04	−0.842 906 83	1.129 933 46	0.061 707 42	4.50E-05
62.201 922 92	−0.214 645 18	1.003 842 84	0.020 414 31	3.04E-06
65.684 540 01	−0.278 617 85	1.025 843 25	0.034 203 85	5.51E-06
67.863 057 28	−0.290 987 41	1.017 485 08	−0.011 281 20	6.19E-06
◊69.327 002 48	−0.297 891 88	0.913 312 09	−0.062 837 37	5.73E-06
◊71.113 788 07	−0.561 667 41	1.044 312 65	0.208 177 21	4.26E-06
74.855 805 47	−0.303 922 50	1.007 744 80	0.017 746 83	8.79E-07
77.313 484 62	−0.311 108 34	0.982 934 92	−0.008 654 56	5.06E-06
◊78.746 766 05	−0.790 881 69	0.575 581 36	−0.303 819 68	1.39E-04
◊80.393 259 12	−0.290 011 65	0.677 267 20	−0.025 341 65	3.99E-05
◊83.891 823 48	−0.480 779 36	0.834 972 21	0.048 754 74	7.22E-05
◊85.818 366 34	−0.411 168 53	0.975 515 35	0.100 039 34	1.05E-05
◊88.577 084 14	−0.627 771 43	0.728 809 37	0.411 147 77	2.73E-05
◊93.034 872 82	−0.121 784 27	0.984 334 04	0.079 976 97	9.37E-05
◊97.584 903 54	−0.419 235 21	0.986 638 23	0.144 082 54	7.12E-05

becomes rather slow [12]. As a second example of periodic orbit quantization by harmonic inversion we therefore study the three-disk scattering system with a short distance ratio $d/R = 2.5$, and thus in a situation where the assumption of the cycle expansion that contributions of long orbits are shadowed by short orbits is no longer a good approximation. The results are presented in figure 4 and table 4. For large L groups of orbits with the same cycle length of the symbolic code strongly overlap and cannot be recognized in figure 4(a). The signal is obtained from periodic orbits with cycle length $n \leqslant 13$. Note that only 356 periodic orbits with $L < 7.5$ are included in the signal (figure 4(a)) whereas the complete set of orbits with cycle length $n \leqslant 13$ consists of 1377 orbits. The resonances obtained by harmonic inversion of the semiclassical recurrence function are in good agreement with results of the cycle expansion [50].

We finally remark that when a symbolic dynamics exists and contributions of long orbits are shadowed by short orbits the cycle expansion techniques are very efficient and, e.g. for the three-disk scattering system with $d \geqslant 6R$, a large number of resonances can be obtained from just eight periodic orbits with cycle length $n \leqslant 4$. Again, we do not aim at competing

with the efficiency of the cycle expansion method in such ideal situations. As already mentioned in section 4, the advantage of periodic orbit quantization by harmonic inversion is its *general* applicability: it does not depend on the existence of a symbolic code and the shadowing of orbits. We have extracted the semiclassical resonances of the three-disk scattering problem directly from the periodic orbits with exactly the same method as the Riemann zeros in section 4 from the primes as 'periodic orbits', for which no symbolic dynamics exists.

7. Conclusion

We have introduced harmonic inversion as a new and general tool for semiclassical periodic orbit quantization. The method requires the complete set of periodic orbits up to a given maximum period as input but does not depend on special properties of the orbits, as, e.g. the existence of a symbolic code or a functional equation. We have demonstrated the wide applicability of the method by applying it to two systems with completely different properties, namely the zeros of the Riemann zeta function and the three-disk scattering problem. Both systems have been treated before by efficient methods, which, however, are restricted to bound ergodic systems or systems with a complete symbolic dynamics. The harmonic inversion technique allows us to solve both problems with one and the same method. Therefore the method can also serve as a tool for, e.g. the semiclassical quantization of systems with mixed regular-chaotic classical dynamics, which is still a challenging and unsolved problem. The signal $C^{\mathrm{sc}}(s)$ can be composed as the sum of a signal related to the irregular part of the classical phase space with periodic orbit amplitudes given by Gutzwiller's trace formula [2] and a signal related to stable [35] or nearly integrable [36] torus structures. It should also be possible to include, e.g. creeping orbits [51], ghost orbit contributions [38, 39, 25], and higher-order $\overline{h}$ corrections [52] into the signal $C^{\mathrm{sc}}(s)$, which can then be inverted to reveal the semiclassical poles. The method can even be used for a semiclassical periodic orbit quantization of systems with non-homogeneous potentials such as the potential surfaces of molecules when a generalized scaling technique [46] is applied.

Acknowledgments

We are grateful to B Eckhardt who kindly communicated to us his periodic orbits for the three-disk scattering system. JM thanks the Alexander von Humboldt-Stiftung for a Feodor-Lynen scholarship and H Taylor and the University of Southern California for their kind hospitality and support.

References

[1] Gutzwiller M C 1967 *J. Math. Phys.* **8** 1979
Gutzwiller M C 1971 *J. Math. Phys.* **12** 343
[2] Gutzwiller M C 1990 *Chaos in Classical and Quantum Mechanics* (New York: Springer)
[3] Berry M V 1986 Riemann's zeta function: A model for quantum chaos? *Quantum Chaos and Statistical Nuclear Physics (Lecture Notes in Physics vol 263)* ed T H Seligman and H Nishioka (Berlin: Springer) pp 1–17
[4] Berry M V and Keating J P 1990 *J. Phys. A: Math. Gen.* **23** 4839
[5] Keating J 1992 *Chaos* **2** 15
[6] Berry M V and Keating J P 1992 *Proc. R. Soc.* A **437** 151
[7] Aurich R, Matthies C, Sieber M and Steiner F 1992 *Phys. Rev. Lett.* **68** 1629
[8] Aurich R and Bolte J 1992 *Mod. Phys. Lett.* B **6** 1691

[9] Bogomolny E B 1992 *Nonlinearity* **5** 805
[10] Cvitanović P and Eckhardt B 1989 *Phys. Rev. Lett.* **63** 823
[11] Artuso R, Aurell E and Cvitanović P 1990 *Nonlinearity* **3** 325
Artuso R, Aurell E and Cvitanović P 1990 *Nonlinearity* **3** 361
[12] Eckhardt B and Russberg G 1993 *Phys. Rev.* E **47** 1578
[13] Eckhardt B, Cvitanović P, Rosenqvist P, Russberg G and Scherer P 1995 Pinball Scattering *Quantum Chaos* ed G Casati and B V Chirikov (Cambridge: Cambridge University Press) pp 405–34
[14] Tanner G, Scherer P, Bogomolny E B, Eckhardt B and Wintgen D 1991 *Phys. Rev. Lett.* **67** 2410
[15] Edwards H M 1974 *Riemann's Zeta Function* (New York: Academic)
[16] Titchmarsh E C 1986 *The Theory of the Riemann Zeta-function* 2nd edn (Oxford: Oxford University Press)
[17] Odlyzko A M 1990 *The* 10^{20}*th Zero of the Riemann Zeta Function and 70 Million of its Neighbours* (AT&T Bell Laboratories)
[18] Bohigas O and Giannoni M J 1984 Chaotic motion and random-matrix theories *Mathematical and Computational Methods in Nuclear Physics (Lecture Notes in Physics vol 209)* ed J S Dehesa *et al* (Berlin: Springer) pp 1–99
[19] Bogomolny E and Keating J 1995 *Nonlinearity* **8** 1115
[20] Main J, Mandelshtam V A and Taylor H S 1997 *Phys. Rev. Lett.* **79** 825
[21] Marple S Jr 1987 *Digital Spectral Analysis with Applications* (Englewood Cliffs, NJ: Prentice-Hall)
[22] Wall M R and Neuhauser D 1995 *J. Chem. Phys.* **102** 8011
[23] Mandelshtam V A and Taylor H S 1997 *Phys. Rev. Lett.* **78** 3274
[24] Mandelshtam V A and Taylor H S 1997 *J. Chem. Phys.* **107** 6756
[25] Main J, Mandelshtam V A and Taylor H S 1997 *Phys. Rev. Lett.* **78** 4351
[26] Delsarte J 1966 *J. Anal. Math. (Jerusalem)* **17** 419
[27] Aurich R, Sieber M and Steiner F 1988 *Phys. Rev. Lett.* **61** 483
[28] Sieber M and Steiner F 1991 *Phys. Rev. Lett.* **67** 1941
[29] Keating J P and Sieber M 1994 *Proc. R. Soc.* A **447** 413
[30] Wintgen D 1988 *Phys. Rev. Lett.* **61** 1803
[31] Ezra G S, Richter K, Tanner G and Wintgen D 1991 *J. Phys. B: At. Mol. Opt. Phys.* **24** L413
[32] Wintgen D, Richter K and Tanner G 1992 *Chaos* **2** 19
[33] Tanner G, Hansen K T and Main J 1996 *Nonlinearity* **9** 1641
[34] Tanner G and Wintgen D 1992 *Chaos* **2** 53
[35] Berry M V and Tabor M 1976 *Proc. R. Soc.* A **349** 101
[36] Tomsovic S, Grinberg M and Ullmo D 1995 *Phys. Rev. Lett.* **75** 4346
[37] Ullmo D, Grinberg M and Tomsovic S 1996 *Phys. Rev.* E **54** 136
[38] Kuś M, Haake F and Delande D 1993 *Phys. Rev. Lett.* **71** 2167
[39] Main J and Wunner G 1997 *Phys. Rev.* A **55** 1743
[40] Ozorio de Almeida A M and Hannay J H 1987 *J. Phys. A: Math. Gen.* **20** 5873
[41] Main J and Wunner G 1998 *Phys. Rev.* E **57** at press
[42] Heller E J 1984 *Phys. Rev. Lett.* **53** 1515
[43] Martens C C, Waterland R L and Reinhardt W P 1989 *J. Chem. Phys.* **90** 2328
[44] Tomsovic S 1991 *J. Phys. A: Math. Gen.* **24** L733
[45] Main J, Wiebusch G, Welge K H, Shaw J and Delos J B 1994 *Phys. Rev.* A **49** 847
[46] Main J, Jung C and Taylor H S 1997 *J. Chem. Phys.* **107** 6577
[47] Eckhardt B, Fishman S, Müller K and Wintgen D 1992 *Phys. Rev.* A **45** 3531
[48] Boosé D, Main J, Mehlig B and Müller K 1995 *Europhys. Lett.* **32** 295
[49] Gaspard P and Rice S A 1989 *J. Chem. Phys.* **90** 2225
Gaspard P and Rice S A 1989 *J. Chem. Phys.* **90** 2242
Gaspard P and Rice S A 1989 *J. Chem. Phys.* **90** 2255
[50] Wirzba A 1997 Private communication
[51] Wirzba A 1992 *Chaos* **2** 77
[52] Gaspard P and Alonso D 1993 *Phys. Rev.* A **47** R3468